Computer Science, Engineering and Technology

Vol: 2(3), September 2024

REST Publisher; ISSN: 2583-9179 (Online)

Website: https://restpublisher.com/journals/cset/

DOI: https://doi.org/10.46632/cset/2/3/8

Optimized U-Net Architecture for Precision in Brain Tumor Segmentation from MRI Scans

***[1]Saritha Dasari, [2]A Rama Mohana Reddy, [3]B. Eswara Reddy**

[1,3] JNTUA, Ananthapuramu, Andhra Pradesh, India.

[2]S.V. University, Tirupati, Andhra Pradesh, India.

**Corresponding author: sarithadasari123@gmail.com*

Abstract: *In contemporary healthcare, precise segmentation of medical pictures is crucial for diagnosis and therapy planning. By automating the hitherto time-consuming human segmentation process, deep learning techniques like CNNs, U-Nets, and Transformers have completely changed this sector. Using deep learning algorithms, this work offers a novel method for brain tumor MRI picture segmentation that tackles the difficulties encountered in contemporary healthcare. We propose an enhanced U-Net model explicitly tailored for this purpose, aiming to improve segmentation precision. Our methodology incorporates feature augmentation techniques during the preprocessing phase, including Contrast Limited Adaptive Histogram Equalization (CLAHE), Multi-histogram Equalization (MHE), and Modified Biorthogonal Histogram Equalization (MBOBHE). Furthermore, we modify the U-Net architecture with a customized layered design to optimize segmentation outcomes. A Convolutional Neural Network (CNN) is employed for post-processing, applying additional convolutional layers to refine the segmentation results. The model demonstrates impressive performance metrics, achieving a recall of 93.66%, accuracy of 97.79%, F-score of 93.15%, and precision of 92.66%. The Dice coefficient's training and validation curves indicate strong generalization capability, with training at approximately 93% and validation at 84%. Despite the model's strengths, challenges remain, particularly concerning false positives, highlighting the need for ongoing refinement. By helping radiologists with precise diagnosis and treatment planning, this work provides the foundation for more accurate and efficient medical image segmentation approaches, which will have a substantial influence on healthcare.*

Keywords: *UNet, Medical Image Segmentation, Healthcare Diagnosis, MRI Images*

1. INTRODUCTION

Brain tumors present a significant health risk and can be life-threatening at any detection stage. They can affect individuals of all ages and genders, with more than 100 distinct types classified as either primary or metastatic. Primary brain tumors, which may be malignant or benign, originate within or near brain structures, while secondary (metastatic) tumors are usually malignant and spread to the brain from other body parts. Survival rates for primary brain tumors vary based on several factors, including age, tumor location, ethnicity, type, and molecular characteristics. Magnetic Resonance Imaging (MRI) has become the preferred method for evaluating various brain abnormalities, providing detailed images without the use of radiation. MRI is especially advantageous compared to CT scans for detecting conditions such as acute ischemia. However, its application in emergency situations is often constrained by the lengthy acquisition process, highlighting the need for quick and accurate diagnoses. Brain MRI segmentation, which involves dividing MRI scans of the brain into distinct regions, is a critical step in medical imaging. It plays a vital role in diagnosing, planning treatments, and monitoring neurological diseases such as brain tumors, multiple sclerosis, Alzheimer's disease, and other brain conditions. Furthermore, quantitative brain analysis—including prenatal diagnosis and early brain development research—needs MRI.

Clinical research has a major issue in brain MRI picture segmentation. In many image analysis applications, particularly in medical imaging, segmentation is essential. In this domain, automated segmentation algorithms typically provide higher

accuracy compared to manual approaches. Quantitative brain analysis requires the automated segmentation of brain tissue from clinical MRI data. This allows for accurate evaluations that support the diagnosis and classification of disorders. Planning for therapy and diagnosing diseases depend on the segmentation method's effectiveness. Differentiating and labeling different anatomical structures, such as white matter (WM), gray matter (GM), CSF, and any diseased regions, is the aim. However, due to variations in brain shape and image intensity around the time of delivery, as well as rapid tissue growth, automatic segmentation of perinatal brain MRI remains difficult. For several analytical tasks linked to brain tumors, including high-resolution reconstruction and cortical surface analysis, accurate and automated brain segmentation is essential. While AI-based medical image segmentation algorithms can attain impressive precision, several radiologists exercise caution. This mistrust comes partially because AI models can occasionally yield errors that clash with expert knowledge, especially when employed across different imaging techniques and diseases. Furthermore, conventional diagnostic techniques are frequently sluggish and error-prone. Due to a lack of specialists in this particular area, there is a growing need for more reliable medical picture segmentation techniques. Traditional segmentation methods, including edge-based, region-based, and thresholding approaches, have difficulties due to biological diversity, pathological variances, and medical image capture limits. Brain MRI segmentation is further complicated by biological variability and the intricacy of brain diseases. One of the challenges that intuitionistic-based clustering algorithms aim to address is pixel value opacity, which is a significant issue in MRI segmentation.

Because U-Net has clear advantages over conventional deep learning (DL), machine learning (ML), and clustering techniques, we apply it in our study for brain MRI segmentation. U-Net's encoder-decoder design is very good at identifying the intricate patterns present in medical images, which makes it possible to segment features with great accuracy. Using its convolutional layers, U-Net autonomously learns the most efficient features, in contrast to traditional ML and clustering methods that rely on manually constructed features and extensive manual tweaks. Furthermore, U-Net's skip connections improve segmentation accuracy by preserving spatial information, especially in complex and changeable anatomical structures. Due to its capacity to efficiently handle issues with motion artifacts and significant anatomical variability, U-Net is particularly well-suited for segmenting brain MRI and fetal brain images.

2. LITERATURE REVIEW

The study "Combining Noise-to-Image and Image-to-Image GANs: Brain MR Image Augmentation for Tumor Detection," by Changhee Han and colleagues, shows that the model's sensitivity increased from 93.67% to 97.48% when a two-step GAN approach was used to detect tumors in the BRATS dataset. In the same year (2019), the same main author partnered with others on a separate study, utilizing the Conditional Progressive Growing of GANs (CPGGANs) model, which boosted the accuracy by 0.64%. This increase was not without a price, though, as the test's accuracy dropped while its sensitivity remained almost 100% and its specificity dropped by 6.84%. This drop in specificity is related to the classifier's detection of fake images.

On the other hand, a 2019 study by Han and colleagues [9] shows that the Conditional Progressive Growing of GANs (CPGGANs) model has enhanced diagnosis sensitivity by 10% while permitting additional false positives that are clinically acceptable. A study named "Enlarged Training Dataset by Pairwise GANs for Molecular-Based Brain Tumor Classification," carried out in 2020 by Ge and colleagues [10], showed that pairwise GANs are a good choice for deep learning models when working with tiny datasets. In this work, original and augmented photos were combined and classified using a dataset; the augmented approach produced better results. By creating a customized U-Net architecture especially for the Intel/Movidius Neural Compute Stick 2 (NCS-2), Shahzad et al. (Shahzad, 2022) achieved notable advancements in medical picture segmentation. Because U-Net has a track record of success in medical picture segmentation—particularly with minimal datasets—it was selected. In order to focus on resource efficiency without sacrificing performance, the redesigned version drastically decreased the amount of parameters from 30 million in the original model to just 0.49 million. The model performed exceptionally well when tested on three medical imaging datasets: brain MRI (BraTs), heart MRI, and Ziehl-Neelsen sputum smear microscopy (ZNSDB). With dice scores of 0.96 for BraTs, 0.94 for heart MRI, and 0.74 for ZNSDB, the model demonstrated good segmentation abilities and allowed for effective NCS-2 platform processing.

In addition to a U-Net-based segmentation model, Akter et al. (2024) designed a deep Convolutional Neural Network (CNN) architecture specifically for the automatic classification of brain pictures into four categories. They carried out thorough assessments on the impact of segmentation on tumor classification in brain MRI images using six benchmark datasets. The study evaluated two classification algorithms and showed better performance than pre-trained models on all datasets. Performance was measured using accuracy, recall, precision, and AUC measures. With a combined dataset, their

classification model demonstrated an astounding 98.7% accuracy, and when paired with segmentation, it reached 98.8%. In addition, the model achieved a 97.7% classification accuracy over the course of the four distinct datasets, demonstrating how well their deep learning methodology improved the segmentation and classification of brain tumors.

An optimization-driven technique for identifying brain cancers from MRI scans was presented by Shiny et al. in 2024. They used filtering approaches and Region of Interest (RoI) extraction to preprocess MRI images, both pre-operative and post-operative. From the preprocessed pictures, tumor segments were generated using a modified U-Net model. Following segmentation, histogram characteristics were retrieved, and a U-Net model trained with the suggested Poor Bird Swarm Optimization algorithm (PRBSA), which combines the Bird Swarm Algorithm (BSA) and the Poor and Prosperous Optimization (PRO) algorithm, was used to classify tumors. Moreover, speeded-up robust features (SURF) on the categorized findings were used to detect pixel changes. The PRBSA-based U-Net model performed well in tumor classification tasks, revealing its usefulness in improving MRI-based brain tumor diagnosis with 94% accuracy, 93.7% sensitivity, and 94% specificity.

A novel 3D Guided Attention-based deep Inception Residual U-Net (GAIR-U-Net) model was presented by Rutoh et al. (2024) to solve the difficulties associated with tumor segmentation in multimodal MRI data. To increase feature representation and the comprehension of spatial context, this model combines attention mechanisms, an inception module, and residual blocks with dilated convolution. The design efficiently captures hierarchical features and complicated patterns by using inception and residual connections, giving it more depth in three dimensions without appreciably increasing processing expenses. The model can learn both local and global information thanks to dilated convolutions, which prioritize important regions and reduce the impact of unimportant characteristics, improving segmentation accuracy and adaptability. On the BraTS 2020 validation dataset, experimental evaluations using the T1-weighted, T1-ce, T2-weighted, and FLAIR sequences performed well, obtaining Dice scores of 0.8796 for the whole tumor (WT), 0.8634 for the tumor core (TC), and 0.8441 for the enhancing tumor (ET).

The novel architecture called Adaptive Cascaded Transformer U-Net (ACTransU-Net) was introduced by Chen et al. (2024) with the goal of MRI brain tumor segmentation. This model successfully captures the fine local details as well as the global context of brain tumors by fusing Transformer mechanisms with dynamic convolution inside a cascaded U-Net architecture. In the first stage, the ACTransU-Net uses two 3D U-Nets for coarse-to-fine segmentation. In the second step, the shallow encoder and decoder are integrated with omni-dimensional dynamic convolution modules. These dynamic modules improve the depiction of local details by varying the convolution kernel settings. Additionally, the second stage's deep encoder and decoder use 3D Swin-Transformer modules to capture long-range dependencies, enhancing the model's ability to describe global tumor structures. The efficacy of the model was validated by experimental results on the BraTS 2020 and BraTS 2021 datasets, which yielded average Dice Similarity Coefficient (DSC) scores of 84.96% and 91.37%, respectively, along with 95th percentile Hausdorff Distance (HD95) values of 10.81 mm and 7.31 mm.

3. PROPOSED METHODOLOGY

This paper introduces a novel approach for brain MRI segmentation using a specially tailored U-Net model. The model's layer configuration has been optimized through extensive experimentation to deliver highly accurate segmentation outcomes. The following sections offer a detailed description of our innovative method. Figure 1 illustrates the complete methodology of our research.

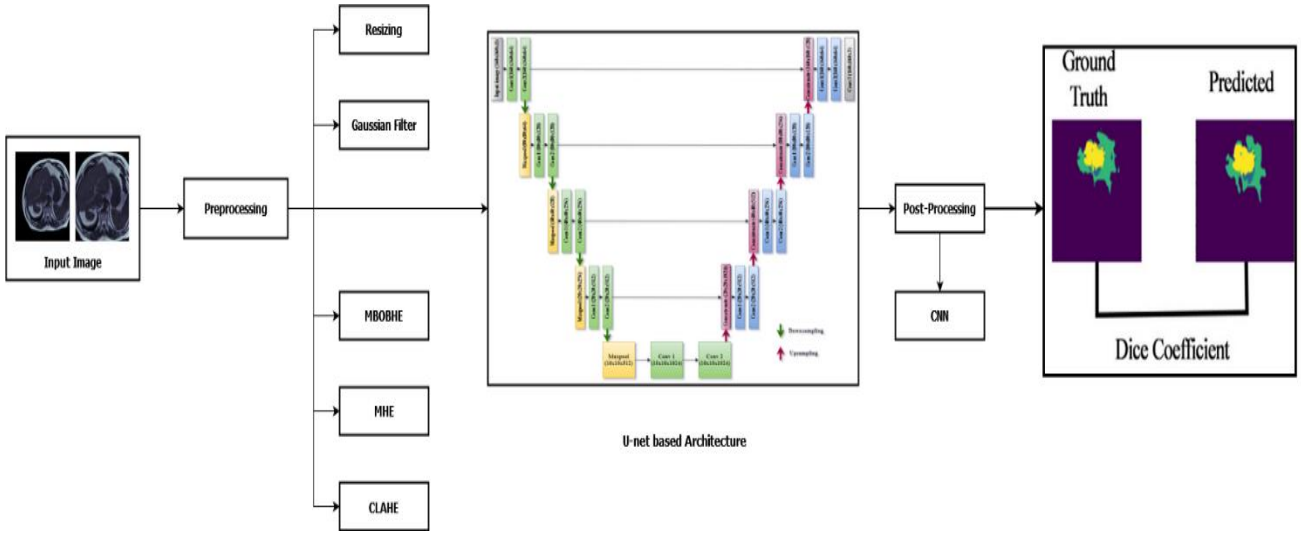

FIGURE 1. The architecture diagram for the proposed model

Dataset Description: A mask that accurately reveals the positions of any tumors is included with every one of the 3,064 brain MRI images in the "Brain MRI Segmentation" Kaggle dataset. With its strong foundation for the creation, improvement, and assessment of advanced machine learning models centered on tumor identification, segmentation, and analysis, this comprehensive dataset is an invaluable tool for medical imaging researchers and practitioners. This dataset has a great deal of promise to improve diagnostic performance and advance automated medical imaging systems because of its extensive annotations. Figure 2 displays an example of data from this collection.

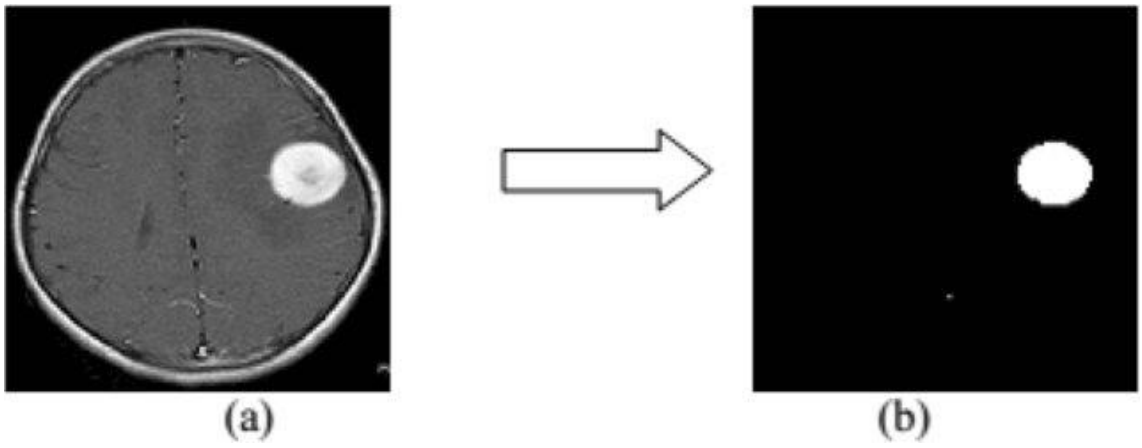

(a) Original Image (b) Corresponding mask indicating tumor location

FIGURE 2. Sample of the dataset

Figure (a) presents the original brain MRI image, showcasing the intricate details of the brain structure. In contrast, Figure (b) features the corresponding mask that highlights the precise location of the tumor within the same image. This mask serves as a crucial tool for identifying and delineating the affected areas, enabling more accurate analysis and segmentation for medical applications.

CNN image post-processing: During the second phase of the fusion model, segmented pictures from the first phase are used in the suggested CNN-based architecture for MRI segmentation. To increase segmentation accuracy, the previously segmented image is loaded into the CNN model. Without segmentation, an image often retains undesired features from less important areas since it includes all background elements, including borders and textures. The convolution and max pooling layers of the proposed CNN model are designed with discrete convolutional blocks (CBs), as follows. This

structure doesn't use any padding and uses a standard stride length.In order to improve segmentation efficiency, we also add a specialized layered design to the U-Net model's architecture.

One max pooling layer and one convolution layer make up the first CB. The max pooling layer is set up as a 2-by-2 configuration, and the first convolution layer uses 32 filters that are three by three in size. Two convolution layers and one max pooling layer make up the second CB. The max pooling layer has 32 filters stacked in a 2-by-2 layout, and the two convolution layers each have 16 filters with a 3-by-3 size. The third CB is made up of two convolution layers and one max pooling layer. The third convolution layer has 16 filters altogether, all of which are 3-by-3 in size, while the max pooling layer once more has a 2-by-2 filter size. Following the third CB, a flattening layer is used, "flattening" the extracted features to reduce the feature space to a single feature vector.

Segmentation Using Proposed U-Net Model: Deep Learning (DL) has improved the analysis of large-scale images, audio, text, video, and tabular data, and has had a significant impact on many different sectors. The necessity for a significant number of medical pictures to train deep learning models was one of the initial obstacles impeding the efficiency of convolutional neural networks (CNNs) in medical image segmentation. The U-Net architecture was created expressly for the purpose of segmenting medical images within smaller datasets in order to address this issue. U-Net produces a pixel-by-pixel annotated image that highlights the segmented region of interest. Unlike traditional CNNs, which often lose critical spatial information needed for segmentation tasks, U-Net preserves both "what" (the content) and "where" (the location) information. Its name derives from its U-shaped design, characterized by the absence of dense layers and the inclusion of only convolutional layers. As an end-to-end fully convolutional network (FCN), U-Net can process images of any size effectively.

In this study, a U-Net model for the automatic segmentation of the stomach, large bowel, and small bowel inside the gastrointestinal (GI) tract has been developed from the ground up. Extensive studies were carried out to ascertain the ideal number and configuration of layers in order to provide the best segmentation results. A combination of max-pooling and convolutional layers make up the U-Net model. The model has a U-shaped structure, as seen in Figure 3, with the decoder on the right and the encoder on the left, following the standard U-Net arrangement. Interestingly, this model does not have any dense layers; instead, it only contains convolution, max-pooling, and transpose convolution layers. This version of U-Net is different from the normal model in that it is made for input images with a resolution of 160 by 160 pixels. It has special layers that are sized to fit the dimensions of the input image.

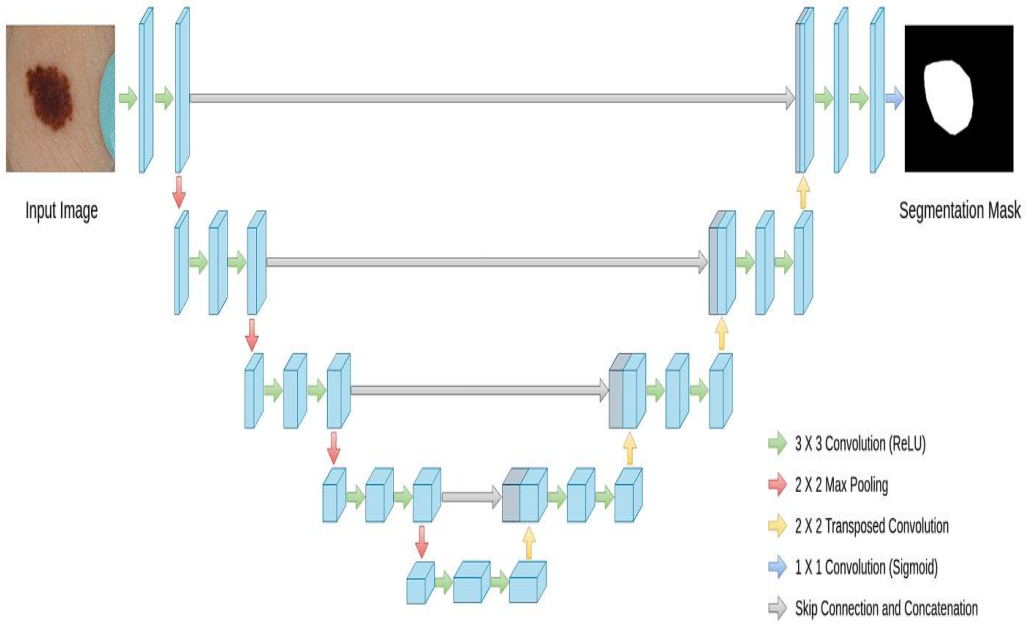

FIGURE 3. Graphical Representation of U-Net Architecture

There are two different methods to approach the architecture. The first path—also referred to as the contraction path or encoder—is in charge of obtaining the image's context. The convolutional layers and max pooling layers in this encoder follow a conventional order. The second approach, called the decoder, is the symmetric expanding path via transposed

convolutions that allows for accurate localization. In this configuration, upsampling is done by the decoder and downsampling by the encoder. The architecture must collect both the contextual information of the input image and high-resolution characteristics in order to perform accurate segmentation jobs.

Hyperparameter Tunning: With a batch size of 32, the models were trained over a period of twenty epochs. The batch size hyperparameter specifies how many samples must be processed before the internal parameters of the model are updated, whereas the epochs parameter shows how many times the complete training dataset has been processed. The learning rate is a critical hyperparameter that controls the model's learning pace. A balanced learning rate is crucial because an excessively high learning rate could cause the model to ignore ideal regions with low loss, while an excessively low learning rate could cause the training process to take longer to reach minimal loss. The learning rate in this investigation was fixed at 0.0001. The Adam optimization algorithm was employed for model compilation, and the ReLU activation function was utilized for all convolutional layers.

4. EXPERIMENTAL ANALYSIS & RESULTS

We have implemented a variety of cutting edge techniques and libraries in our experimental setup for brain tumor detection and segmentation. For tasks like feature extraction, preparing data, and evaluating model performance metrics, we use Scikit-learn (sklearn) to develop and evaluate machine learning models. We employ Matplotlib to visualize MRI images, masks, and segmentation results, which facilitates the efficient interpretation and communication of our results. Google Colab provides a scalable and cooperative computing environment that makes it easy to share and execute code while utilizing high-performance computing resources that are necessary for training intricate models on large datasets. This coordinated strategy guarantees a cooperative, fruitful, and repeatable research process while improving the validity and dependability of our experimental outcomes.
To enable reliable assessment and model generalization, we separated the dataset into training, validation, and test sets in our experimental design. Sixty-one photos and masks each for validation and testing are included in the dataset, which has 1,840 images and masks set aside for training. Our machine learning models are trained, tuned, and tested more effectively thanks to this stratified partitioning, which guarantees precise performance evaluation and optimization. We assessed the effectiveness of our tumor detection and segmentation models using a set of evaluation metrics.

Analysis of Dice Coefficient: When evaluating the similarity of two samples, especially the predicted and ground truth masks of brain tumors in MRI images, one often used metric is the dice coefficient. The formula for calculating it is the ratio of the total area of both masks to twice the location where the expected and actual masks connect. Essentially, more overlap and alignment between the estimated and genuine tumor locations is indicated by a higher Dice coefficient.

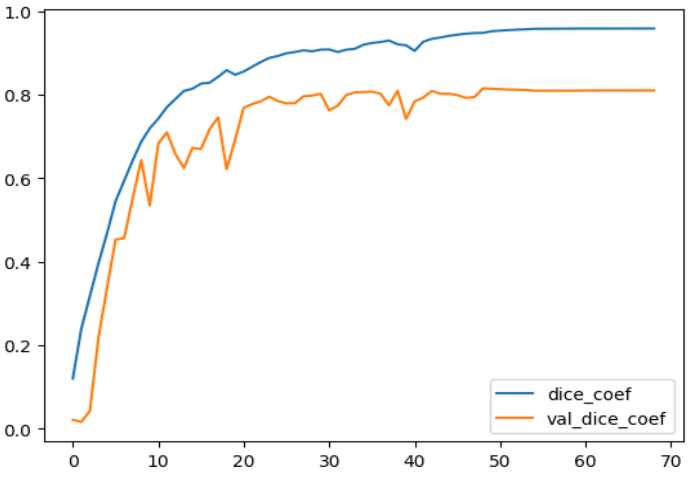

FIGURE 4. Dice Coefficient of the proposed model

The curve is displayed in Figure 4. The provided graph illustrates the performance of a model evaluated through the Dice coefficient over the course of 70 epochs. The blue line represents the training Dice coefficient, which shows a steady increase, approaching a value of 1. This indicates that the model is effectively learning to segment the data as training progresses. In contrast, the orange line reflects the validation Dice coefficient, which exhibits a more fluctuating behavior.

While it initially rises, it stabilizes at a lower value than the training coefficient, suggesting that the model may be experiencing some overfitting. This discrepancy between training and validation metrics underscores the importance of implementing strategies to enhance generalization, such as early stopping or regularization, to improve the model's performance on unseen data.

The model's capacity to precisely identify and segment tumors in MRI images that had never been seen before was demonstrated by the validation set, which yielded a Dice coefficient of about 84%, suggesting a strong performance. The model consistently performs well on both training and validation sets, demonstrating strong generalization capabilities. However, minimizing any disparities in these performance measures should be the main goal of future modifications and studies.

Generalization analysis of the proposed model: In this work, we evaluate a critical component of model generalization for the recognition and classification of brain cancers using MRI images. "Generalization" is the ability of a model to apply learnt patterns and characteristics to real-world situations; it is the process of interpreting data that is outside of its training set and has not yet been seen before. The training and validation loss, as well as the accuracy, are shown in Figures 5 and 6.

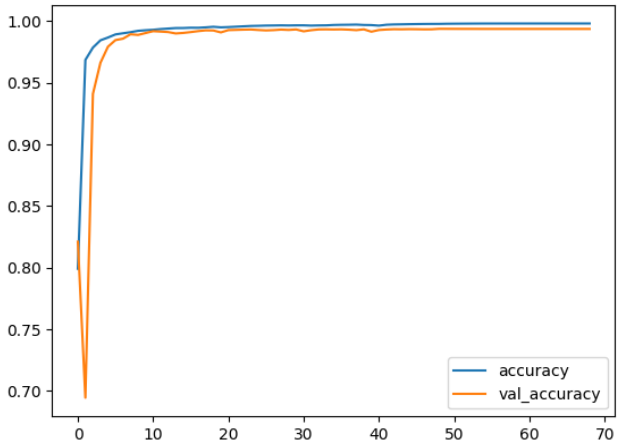

FIGURE 5. Training and validation accuracy

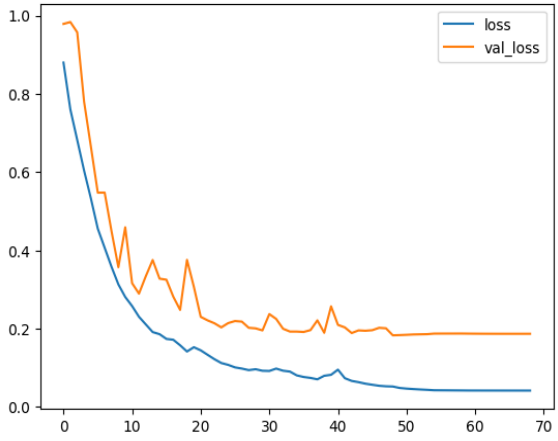

FIGURE 6. Training And validation loss

Figure 5 presents the training and validation accuracy of the model over the course of 70 epochs. The blue line indicates the training accuracy, which shows a steady upward trend, ultimately reaching an accuracy close to 1. This suggests that the model effectively learns to classify the data throughout the training process. The orange line represents the validation accuracy, which closely follows the training accuracy and also approaches a value of 1, indicating that the model generalizes well to the validation dataset. The proximity of both accuracy lines suggests minimal overfitting, as the model maintains high performance on both the training and validation datasets, reinforcing its potential for reliable real-world application in brain tumor identification and segmentation in MRI images.

Figure 6 illustrates the training and validation loss curves over 70 epochs. The blue curve depicts the training loss, while the orange curve represents the validation loss. At the beginning, both losses decrease significantly, indicating that the model is effectively learning. However, after approximately 20 epochs, the validation loss begins to fluctuate and levels off, whereas the training loss continues to decline steadily. This pattern suggests that the model might be overfitting to the training data, as it continues to improve on the training set while struggling to generalize to the validation set beyond this point.

Performance of the proposed model: We assessed our model's performance using various metrics, including test accuracy, F-score, precision, and recall. The results for the proposed U-Net model are summarized in Table 1. The precision score was 92.66%, demonstrating the model's effectiveness in minimizing false positives—areas wrongly identified as tumors—and its competence in accurately detecting true brain tumor cases. The recall rate was 93.65%, indicating that the model successfully identifies most actual positive cases, resulting in very few undetected tumors. This is crucial in medical diagnostics, as failing to detect a tumor can have serious consequences for patient outcomes. 93.15% was the recorded F-score, which is the harmonic mean of recall and precision. This statistic offers an all-encompassing perspective on the model's efficacy by evaluating its capacity to detect genuine positives while reducing false positives. The results demonstrate a great balance between precision and recall. Moreover, the model demonstrated a high percentage of correctly identified occurrences (both true positives and true negatives) with an exceptional total accuracy of 97.79% on the test set.

This exceptional accuracy is a result of the model's robust ability to reliably classify both tumor and non-tumor regions, as well as its consistent performance in a variety of settings.

TABLE 1. Performance of the proposed U-Net model

Evaluation Metrics	Performance
Recall	93.65 %
Precision	92.66 %
Accuracy	97.79 %
F-score	93.15 %

Visual analysis of the segmentation: In the results section of our brain MRI segmentation analysis, we showcased the performance of our model using a series of images that illustrate both accurate and inaccurate segmentations. Figure 7 provides a visualization of these results. In the first two images, the actual mask overlays are clearly displayed on the MRI scans, demonstrating the model's capability to accurately identify and segment tumor regions. The effectiveness of the model in distinguishing tumor tissues from surrounding brain structures is evident in how closely the segmented areas align with the ground truth masks. This precise segmentation is crucial for ensuring that tumor regions are accurately identified without including non-tumor areas, which is essential for proper diagnosis and treatment planning.

However, the last image reveals a segmentation error. While the model correctly identifies the primary tumor site, it also mistakenly marks an adjacent area as a tumor. This misclassification indicates a false positive in the model's predictions, highlighting a potential for misinterpretation of MRI images or unnecessary treatments. The reasons for this error could include the complexity and variability of brain tumor appearances in MRI scans, the quality of the training data, and potential overfitting to specific features present in the training set. To address these issues, the model needs enhancements, such as incorporating a more diverse range of examples into the dataset, applying advanced regularization techniques, and fine-tuning the model's hyperparameters to improve generalization. Future research should focus on strategies to reduce these errors.

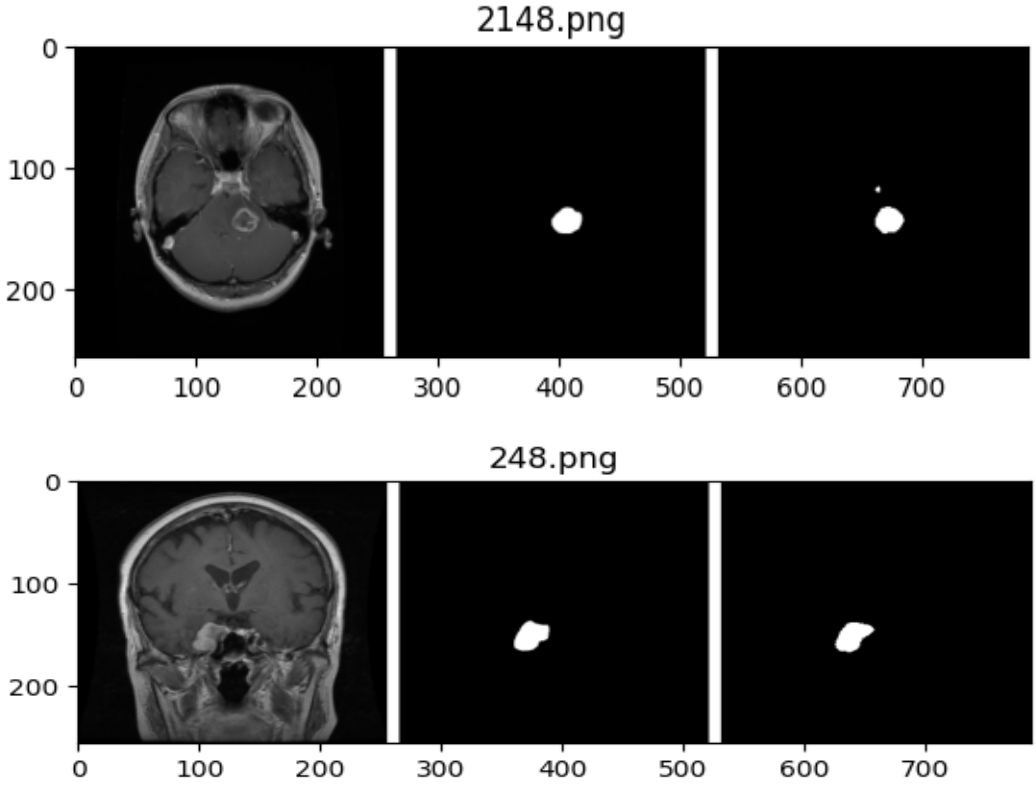

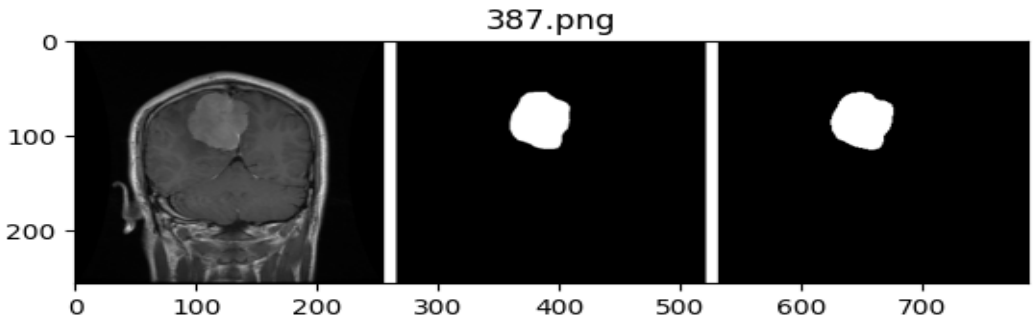

FIGURE 7. Visual analysis of segmented images

5. CONCLUSION

In this work, we use deep learning algorithms to present a fresh solution to the problems associated with brain tumor MRI picture segmentation in modern healthcare. We present a refined U-Net model created especially to increase the accuracy of MRI segmentation of brain tumors. During the picture preprocessing step of our procedure, we apply feature augmentation techniques such as Contrast Limited Adaptive Histogram Equalization (CLAHE), Multi-histogram Equalization (MHE), and Modified Biorthogonal Histogram Equalization (MBOBHE). In order to improve segmentation efficiency, we also add a specialized layered design to the U-Net model's architecture. Finally, we implement a Convolutional Neural Network (CNN) for post-processing, which includes additional convolutional layers to further optimize the segmentation results. Our model achieved impressive performance metrics, including a recall rate of 93.66%, accuracy of 97.79%, F-score of 93.15%, and precision of 92.66%. The training and validation curves for the Dice coefficient showed slight discrepancies, with training reaching approximately 93% and validation at 84%, indicating strong generalization capability. There are numerous avenues for further research. This work lays the groundwork for more precise and effective medical image segmentation techniques, which could greatly influence healthcare by assisting radiologists in making accurate diagnoses and formulating treatment plans. In summary, our evaluation of the U-Net model for brain MRI segmentation highlights its significant potential for accurately identifying and segmenting tumor regions.The evaluation metrics, which include high precision, recall, F-score, and overall accuracy, demonstrate the model's effectiveness in distinguishing between tumor and non-tumor areas—an essential factor for precise diagnosis and treatment planning. Visualization results further confirm the model's performance, highlighting its strengths in accurately matching segmented areas with ground truth masks. However, challenges persist, particularly with instances of false positives that may result in misinterpretations of MRI images and unnecessary interventions. These inaccuracies underscore the complexities involved in identifying brain tumors and emphasize the need for continuous refinement of the model. Future research should prioritize enhancing segmentation accuracy by diversifying the training dataset, applying advanced regularization techniques, and optimizing hyperparameters.O verall, while the model lays a solid foundation for brain tumor segmentation, ongoing efforts to address its limitations will improve its reliability and effectiveness in clinical applications, ultimately leading to better patient outcomes.

REFERENCES

[1]. Abdelatty, M. A. (2024). Magnetic resonance imaging of pilonidal sinus disease: interobserver agreement and practical MRI reporting tips. European Radiology, 115--125.

[2]. Agarap, A. F. (2018). Deep learning using rectified linear units (relu). arXiv preprint arXiv:1803.08375.

[3]. Akter, A. a. (2024). Robust clinical applicable CNN and U-Net based algorithm for MRI classification and segmentation for brain tumor. Expert Systems with Applications, 122347.

[4]. Shiny, RS Ajila, G. Ganan Shini, M. Ramachandran, Chinnasami Sivaji, and Manjula Selvam. "Characteristics of Modern Landscape Architecture and Its Planning Methods." *Sustainable Architecture and Building Materials* 1, no. 1 (2022): 21-31.

[5]. Al Garea, S. a. (2024). Image Segmentation Methods: Overview, Challenges, and Future Directions. In 2024 Seventh International Women in Data Science Conference at Prince Sultan University (WiDS PSU) (pp. 56--61).

[6]. Altmann, S. a. (2024). Ultrafast brain MRI with deep learning reconstruction for suspected acute ischemic stroke. Radiology, e231938.

[7]. Arora, J. a. (2024). Conditional spatial biased intuitionistic clustering technique for brain MRI image segmentation. Frontiers in Computational Neuroscience, 1425008.

[8]. Cai, Z. a.-M. (2024). Enhancing Generalized Fetal Brain MRI Segmentation using A Cascade Network with Depth-wise Separable Convolution and Attention Mechanism. arXiv preprint arXiv:2405.15205.

[9]. Chen, B. a. (2024). Adaptive cascaded transformer U-Net for MRI brain tumor segmentation. Physics in Medicine \& Biology, 115036.
[10]. Nanjundan, Prabakaran, M. Ramachandran, Chandraseker Raja, and Chinnasami Sivaji. "Classification of the Architecture Using IBM SPSS Statistics."
[11]. Ciceri, T. a. (2024). Fetal brain mri atlases and datasets: a review. NeuroImage, 120603.
[12]. Desale, P. a. (2024). Navigating Neural Landscapes: A Comprehensive Review of Magnetic Resonance Imaging (MRI) and Magnetic Resonance Spectroscopy (MRS) Applications in Epilepsy. Cureus.
[13]. Fidon, L. a. (2024). A Dempster-Shafer approach to trustworthy AI with application to fetal brain MRI segmentation. IEEE transactions on pattern analysis and machine intelligence.
[14]. G{\"o}rgec, B. a. (2024). MRI in addition to CT in patients scheduled for local therapy of colorectal liver metastases (CAMINO): an international, multicentre, prospective, diagnostic accuracy trial. The Lancet Oncology, 137--146.
[15]. Huang, S. a. (2020). Medical image segmentation using deep learning with feature enhancement. IET Image Processing, 3324-3332.
[16]. Saritha Dasari, A Rama Mohana Reddy, B. Eswara Reddy, “Advanced U-Net Model for Precise Brain Tumor Segmentation in MRI Images”, REST Journal on Data Analytics and Artificial Intelligence 3(2),June 2024, 75-88.
[17]. Kurinjimalar Ramu, M. Ramachandran, Vidhya Prasanth, and Prabakaran Nanjundan. "Application of Mobile Learning Methods in the 21 st Century." *Journal on Innovations in Teaching and Learning* 1 (2022): 1.
[18]. Hum, Y. C. (2014). Multiobjectives bihistogram equalization for image contrast enhancement. Complexity, 22-36.
[19]. Ishfaq, M. A. (2023). Brain tumor classification utilizing deep features derived from high-quality regions in MRI images. Biomedical Signal Processing and Control, 104988.
[20]. Kiran, L. a. (2024). An enhanced pattern detection and segmentation of brain tumors in MRI images using deep learning technique. Frontiers in Computational Neuroscience, 1418280.
[21]. Kumar, P. R. (2024). Automated human brain tissue segmentation from clinical MRI images for improved neurological diagnosis and treatment planning. Intelligent Medicine.
[22]. Kumar, P. R. (2024). Automated human brain tissue segmentation from clinical MRI images for improved neurological diagnosis and treatment planning. Intelligent Medicine.
[23]. Mahajan, A. a. (2024). Neuroimaging: CT Scan and MRI. In Principles and Practice of Neurocritical Care (pp. 189--215). Springer.
[24]. Nehra, M. a. (2021). Nanobiotechnology-assisted therapies to manage brain cancer in personalized manner. Journal of Controlled Release, 224--243.
[25]. Reddy, S. a. (2024). Region based image segmentation to improve accuracy of currency images compared with edge based segmentatio. In AIP Conference Proceedings.
[26]. Reza, A. M. (2004). Realization of the Contrast Limited Adaptive Histogram Equalization (CLAHE) for Real-Time Image Enhancement. Journal of VLSI signal processing systems for signal, image and video technology.
[27]. Rutoh, E. K. (2024). GAIR-U-Net: 3D guided attention inception residual u-net for brain tumor segmentation using multimodal MRI images. Journal of King Saud University-Computer and Information Sciences, 102086.
[28]. Shahzad, O. A. (2022). Implementation of a Modified U-Net for Medical Image Segmentation. IEEE, 4593--4597.
[29]. Sharif, M. a. (2024). Brain tumor segmentation and classification by improved binomial thresholding and multi-features selection. Journal of ambient intelligence and humanized computing, 1--20.
[30]. Shi, H. C. (2004). A simple and effective histogram equalization approach to image enhancement. Digital Signal Processing, 158-170.
[31]. Shiny, K. (2024). Brain tumor segmentation and classification using optimized U-Net. The Imaging Science Journal, 204--219.
[32]. Solanki, S. a. (2023). Brain Tumor Detection and Classification Using Intelligence Techniques: An Overview. IEEE Access, 12870-12886.
[33]. Soppari, K. a. (2024). A survey on brain MRI segmentation. World Journal of Advanced Research and Reviews, 1702--1710.
[34]. Yellu, R. R. (2024). edical Image Analysis-Challenges and Innovations: Studying challenges and innovations in medical image analysis for applications such as diagnosis, treatment planning, and image-guided surgery. Journal of Artificial Intelligence Research and Applications, 93--100.
[35]. Zhang, A. S.-S. (2017). Complete prevalence of malignant primary brain tumors registry data in the United States compared with other common cancers, 2010. Neuro-oncology, 726--735.
[36]. Zhang, Y. a. (2024). Interactive medical image annotation using improved Attention U-net with compound geodesic distance. Expert systems with applications, 121282.
[37]. Zhang, Z. (2018). Improved Adam Optimizer for Deep Neural Networks. In 2018 IEEE/ACM 26th International Symposium on Quality of Service (IWQoS) (pp. 1-2).

